

(1969).

- ⁶M. L. Cohen and V. Heine, in Ref. 3, p. 37.
- ⁷I. V. Abarenkov and V. Heine, *Phil. Mag.* **12**, 529 (1965); V. Heine and I. V. Abarenkov, *ibid.* **9**, 451 (1964).
- ⁸R. W. Shaw, Jr. and W. A. Harrison, *Phys. Rev.* **163**, 604 (1967).
- ⁹J. B. Pendry, *J. Phys. C* **4**, 427 (1971).
- ¹⁰V. Heine, in Ref. 3, p. 1.
- ¹¹W. Shyu, J. H. Wehling, M. R. Cordes, and G. D. Gaspari, *Phys. Rev. B* **4**, 1802 (1971).
- ¹²Additional calculations are currently being carried out by M. Appapillai and V. Heine using optimized-model-potential programs (Refs. 2 and 4).
- ¹³W. A. Harrison, *Phys. Rev.* **181**, 1036 (1969).
- ¹⁴J. A. Moriarty, *Phys. Rev. B* **1**, 1363 (1970); and (unpublished).
- ¹⁵A. R. Williams and D. Weaire, *J. Phys. C* **3**, 386 (1970).
- ¹⁶R. W. Shaw, Jr., *J. Phys. C* **3**, 1140 (1970).
- ¹⁷K. S. Singwi, M. P. Tosi, R. H. Land, and A. Sjölander, *Phys. Rev.* **176**, 589 (1968); *Phys. Rev. B* **1**, 1044 (1970).
- ¹⁸F. Toigo and T. O. Woodruff, *Phys. Rev. B* **2**, 3958 (1970).
- ¹⁹P. S. Ho, *Phys. Rev.* **169**, 523 (1968); *Phys. Rev. B* **3**, 4035 (1971).
- ²⁰N. W. Ashcroft, *Phys. Letters* **23**, 48 (1966).
- ²¹R. W. Shaw, Jr. and V. Heine, *Phys. Rev. B* **5**, 1646 (1972).
- ²²J. M. Ziman, *Advan. Phys.* **13**, 89 (1964).
- ²³P. W. Anderson (unpublished).
- ²⁴A. Meyer and W. H. Young, *Phys. Rev. Letters* **23**, 973 (1969).
- ²⁵M. A. Ball, *J. Phys. C* **2**, 1248 (1969); M. M. Islam and M. A. Ball, *Phil. Mag.* **22**, 1227 (1971).
- ²⁶V. Heine and M. J. G. Lee, *Phys. Rev. Letters* **27**, 811 (1971).
- ²⁷M. J. G. Lee and V. Heine, *Phys. Rev. B* (to be published).
- ²⁸W. A. Harrison, *Solid State Theory* (McGraw-Hill, New York, 1970).
- ²⁹J. M. Ziman, *Proc. Phys. Soc. (London)* **91**, 701 (1967).
- ³⁰L. I. Schiff, *Quantum Mechanics* (McGraw-Hill, New York, 1955).
- ³¹R. W. Shaw, Jr., thesis (Stanford University, 1968) (unpublished).
- ³²J. Friedel, *Phil. Mag.* **43**, 153 (1952).
- ³³See, for example, D. L. Price, K. S. Singwi, and M. P. Tosi, *Phys. Rev. B* (to be published); and references quoted in Heine and Weaire (Ref. 3).
- ³⁴L. Hedin and R. Sjöström, *Nat. Bur. Std. Spec. Publ.* **323** (1971).
- ³⁵L. Pauling, *The Nature of the Chemical Bond* (Cornell U. P., Ithaca, 1940).
- ³⁶R. W. Shaw, Jr., *Phys. Rev. B* **5**, 4856 (1972).
- ³⁷A. Meyer, I. H. Umar, and W. H. Young, *Phys. Rev. B* **4**, 3287 (1971).
- ³⁸R. J. Gambino and P. E. Seiden, *Phys. Rev. B* **2**, 3571 (1971).
- ³⁹P. B. Allen and M. L. Cohen, *Phys. Rev.* **187**, 525 (1969).
- ⁴⁰W. L. McMillan, *Phys. Rev.* **167**, 331 (1968).
- ⁴¹B. W. Roberts, *Natl. Bur. Std. Tech. Note* **482** (1969).
- ⁴²B. T. Matthias, *Am. Scientist* **58**, 80 (1970), and references contained therein.
- ⁴³M. L. Cohen and T. K. Bergstresser, *Phys. Rev.* **141**, 789 (1966).
- ⁴⁴J. C. Phillips, *Rev. Mod. Phys.* **42**, 317 (1970).

Pressure Effect on the Diffusion of Carbon in α -Iron

J. F. Cox and C. G. Homan

Benet Weapons Laboratory, Watervliet Arsenal, Watervliet, New York 12189

(Received 17 January 1972)

Diffusion of carbon in α -iron has been measured in the temperature range of 823 to 1000 °K and at pressures up to 6 kbar, using a radio-tracer diffusion couple technique. A large activation volume for the diffusion of carbon in α -iron was obtained as compared to the zero activation volume found at room temperature by relaxation techniques. This volume is considerably larger than the activation volume Hilliard and Tully found for carbon diffusion in austenite but is nearly equal to the activation volume for austenite decomposition determined by Hilliard and Cahn and by Nilan.

INTRODUCTION

Bosman *et al.*¹ and Bass and Lazarus² have shown that the activation energy for diffusion of carbon in α -iron, as determined by magnetic and anelastic relaxation techniques, is independent of pressure up to about 6 kbar. The most recent determination³⁻⁵ of carbon diffusion in α -iron at tem-

peratures above 723 °K shows quite clearly that low-temperature diffusivities obtained through relaxation measurements cannot be extrapolated to obtain high-temperature diffusivities.

The disagreement at high temperature between experimental diffusivities and diffusivities predicted from low-temperature relaxation measurements suggests that it may be impossible to pre-

TABLE I. Analysis of Battelle-iron Specimen 33E, lot 8 as received, from which all diffusion couples were made. This analysis provided by Dr. G. Rengstorff of Battelle Memorial Institute by direction of Dr. K. Blickwede, Chairman of the AISI subcommittee for pure-iron research.

Metallic impurities			
Aluminum	15ppm	Magnesium	< 5
Antimony	< 5 nd ^a	Manganese	< 0.1
Arsenic	< 5 nd	Molybdenum	< 5 nd
Beryllium	< 0.2	Nickel	20
Boron	< 5	Phosphorus	9
Cadmium	< 5 nd	Silicone	10
Calcium	< 10 nd	Tin	< 5 nd
Chromium	5	Titanium	< 1 nd
Cobalt	5	Tungsten	< 5 nd
Copper	7	Vanadium	< 1 nd
Lead	< 1 nd	Zinc	< 10 nd
		Zirconium	< 1 nd
Interstitials			
Carbon	< 10 ppm	(combustion)	
Oxygen	11	(vacuum fusion)	
Nitrogen	< 2	(vacuum fusion)	
Hydrogen	< 0.1	(photometric)	

^and means not detected. Detection limits given.

dict the effect of pressure on the diffusivity of carbon in α -iron at high temperatures from the results obtained with relaxation techniques. In this paper we present results of direct measurements of carbon diffusion in α -iron at high temperature and pressures.

EXPERIMENTAL PROCEDURE

Diffusion couples consisting of a segment of high-purity Battelle iron welded to a segment of Battelle iron doped with C^{14} were prepared as previously described.⁴ The chemical analysis provided with the Battelle iron is given in Table I. Decarburization and/or contamination of diffusion couples by impurities present in argon- and helium-pressure media were prevented by electroplating all specimens with copper.

A schematic of the high-pressure-annealing assembly is shown in Fig. 1. The pressure-bomb closure was cooled by passing water through a copper coil silver soldered to the closure. In addition to reducing the possibility of closure failure, the cooling coil provided a region in the bomb which was several hundred centigrade degrees below the diffusion-anneal temperatures.

The heated end of the vessel was immersed in a furnace with two independently controlled windings. Two chromel-alumel thermocouples were mounted approximately 5 cm apart on the outer low-pressure surface of the pressure vessel. A temperature difference between the two thermocouples of less

than 1 °C was continuously maintained by manual adjustment of the power input to the separate windings.

Temperature calibration runs at 1 atm showed that, after a suitable warm-up period, the diffusion-anneal zone was characterized by axial temperature gradients no greater than 0.4 °C/cm and radial temperature gradients no greater than 0.1 °C/cm. Calibration runs also showed that the external thermocouples agreed to within normal experimental error with thermocouples placed inside the pressure vessel.

A more significant evaluation of the agreement between the external-thermocouple readings and the actual temperature inside the pressure vessel was obtained by heating lead, aluminum, and silver at high pressure to their melting temperatures. Melting-point samples were held in the cooled closure end of the inverted pressure vessel. The other end of the pressure vessel was heated to within ± 0.5 °C of the desired experimental temperatures. When temperature stability was achieved, the pressure vessel was rotated 180° to cause the sample to fall into the hot zone and was then returned to the horizontal plane by a 90° reverse rotation. The specimen was held at temperature and pressure for a short period after which the power to the furnace was interrupted. Evidence of melting was obtained by optical examination of heated specimens.

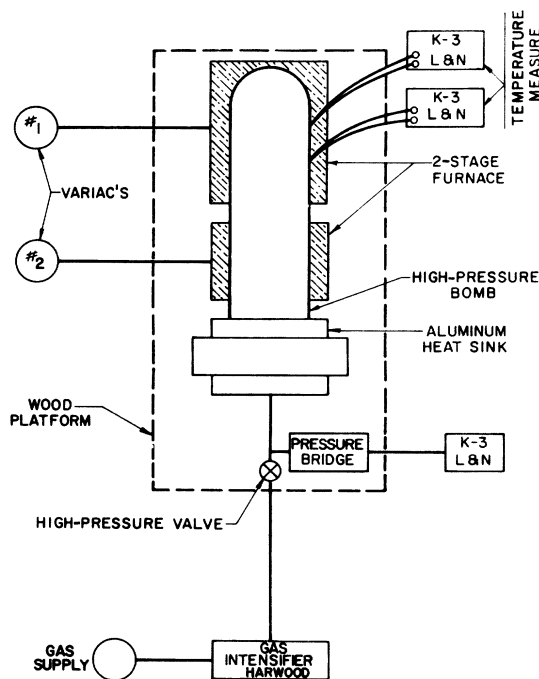


FIG. 1. Schematic of high-pressure-diffusion apparatus.

TABLE II. Pressure calibration of thermocouples.

Metal	Room- pressure melting point (°C)	γ	c	High- pressure theoret. (°C)	Melting point expt. (°C)	Pressure (atm)	T_{error} (°C)
Pb	327.4	2.35	1.41	328.3	328.6	1530	+0.3
Al	659.7	2.1	1.28	663.3	662.6	2000	-0.7
Ag	960.8	2.2	1.27	966.6	962.8	2000	-1.8

Strong⁶ has shown that the Simon semiempirical fusion-curve formula⁷ may be used in the Clausius-Clapeyron equation to obtain a melting-point formula:

$$\frac{dP}{dT} = \frac{L}{T_0 \Delta V} = \frac{ca}{T_0}, \quad (1)$$

where P is the applied pressure in atm, T_0 is the melting temperature at zero pressure, T is the melting point at pressure P , a was considered by Simon to be related to the internal pressure (Strong finds a to be about 400 000 atm), c was a constant exponent of the Simon theory, L is the latent heat of fusion, and ΔV is the volume change of melting.

Salter⁸ and Gilvarry⁸ showed that Simon's exponent c is related to Grüneisen's constant γ by

$$c = \frac{6\gamma + 1}{6\gamma - 2}. \quad (2)$$

Theoretical values of the increase of the melting points with pressure were calculated from this theory and compared to the experimentally determined values of the melting-point temperatures for Pb, Al, and Ag. Assuming the above theory to be exact, it was possible to estimate the temperature error to be no more than 0.5 °C at 327 °C to 2.0 °C at 960 °C. The theoretical and measured values of the melting-point temperature of the above metals are shown in Table II.

All thermocouples were repeatedly calibrated against a Pt-Pt 10-at.% Rh standard thermocouple. All thermal emf's were measured against an ice-bath reference junction using an L&NK-3 potentiometer.

Temperature measurements during the high-pressure anneals were made every few minutes. The reported anneal temperatures are time-weighted mean values. Temperature deviations during all runs were small enough so that a more refined correction procedure was unnecessary.

Pressure measurements were obtained with a transducer which utilized a four-unit strain-gauge bridge. The transducer was repeatedly calibrated to 6.7 kbar against a free-piston high-pressure calibration unit and a calibrated manganin coil. Immediately before each anneal, the transducer was recalibrated against a Heise gauge up to the maximum precharge pressure of about 2 kbar.

Higher-pressure levels reported in this investigation were obtained by precharging at room temperature and heating the sealed bomb to the desired anneal temperature. A Tem Press Research, State College, Pa. Model No. MRA-414B bomb was used in this experiment.

As shown in Fig. 1, the high-pressure-annealing apparatus was mounted on a rotatable platform. The pressure vessel was pressurized, sealed, and heated to the desired annealing temperature. The heat-up was performed with the bomb axis in the horizontal plane and with the sample positioned in the cool closure end. After the desired temperature was obtained in the bomb, a rotation to the vertical plane dropped the sample into the hot zone. Entry of the sample into the hot zone was indicated by a measurable change in system pressure and temperature. The pressure vessel was immediately returned to the horizontal plane with pressure and temperature recovery indicating a total heat-up time of several minutes. Upon completion of the anneal, samples were removed from the hot zone by appropriate rotation of the pressure bomb.

Penetration profiles were obtained by grinding off known thicknesses of material and counting the C^{14} β particles emitted from the exposed surface. Counting was accomplished using an end-window Geiger-Muller tube as previously described⁴ or a gas-flow proportional counter designed to accommodate the diffusion specimens. The proportional counter had a counting sensitivity of about 45% which permitted measurements of low-activity specimens.

Proper operation of the gas-flow proportional counter was established by obtaining several profiles using both counting systems. Operation of all counting equipment was checked at regular intervals by subjecting counting data to χ^2 statistical tests.

RESULTS

Experimental conditions were such that concentration profiles could be analyzed using the Grube-Jedele solution to the diffusion equation. This solution, which applies when the cementite solubility limit is not exceeded in any part of the couple, is

$$\frac{2(c_x - c_b)}{(c_0 - c_b)} = \operatorname{erfc} \left(\frac{x}{2(Dt)^{1/2}} \right), \quad (3)$$

where c_x is the carbon concentration at x cm from the original interface, c_b is the initial carbon concentration on the low-carbon-concentration side of the couple, D is the diffusivity in cm^2/sec , and t is the anneal time in seconds. If the assumption is made that the carbon specific activity remains constant (i.e., no measurable isotope effect) during a measurement, then the carbon concentration ratio in Eq. (3) may be replaced by the ratio of count

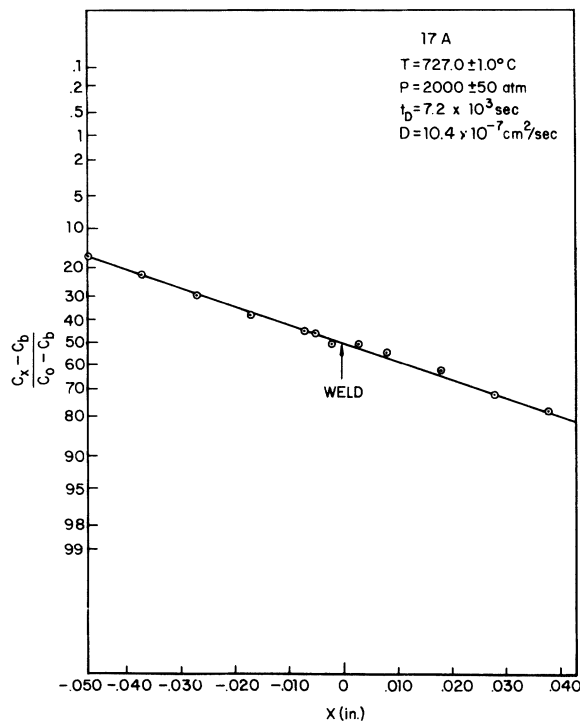


FIG. 2. Plot of concentration ratio versus distance from weld on probability paper.

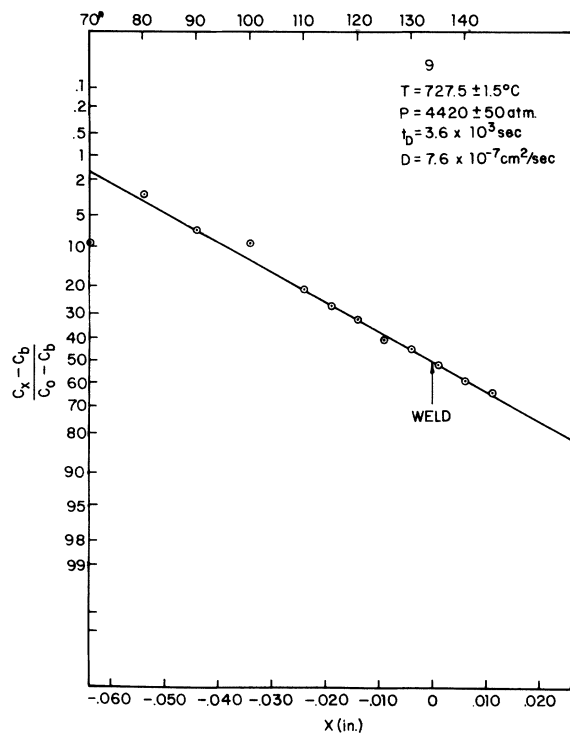


FIG. 3. Plot of concentration ratio versus distance from weld on probability paper.

rates.

Typical penetration profiles, as plotted on probability paper, are shown in Figs. 2-5. The straight lines obtained from these plots indicated that the diffusivity is independent of carbon concentration over the concentration range of these samples. Diffusivities (and other pertinent data) obtained from the penetration plots are summarized in Table III.

DISCUSSION

Samples 16, 20A, and 20B were annealed at essentially atmospheric pressure. Diffusivities obtained from these samples are in good agreement with the following relationship obtained from measurements of diffusion of carbon in α -iron at atmospheric pressure⁴:

$$D = 0.008 \exp\left(-\frac{19800 \text{ cal mole}^{-1} \text{ }^\circ\text{K}^{-1}}{RT}\right) + 2.2 \exp\left(-\frac{29300 \text{ cal mole}^{-1} \text{ }^\circ\text{K}^{-1}}{RT}\right). \quad (4)$$

The pressure variation of carbon diffusion in α -iron at 889 and 1000 $^\circ\text{K}$ is shown in Figs. 6 and 7, respectively. These data were analyzed using two approaches.

The usual empirical approach of determining the slope of $\ln D$ -versus- P plots and calculating "acti-

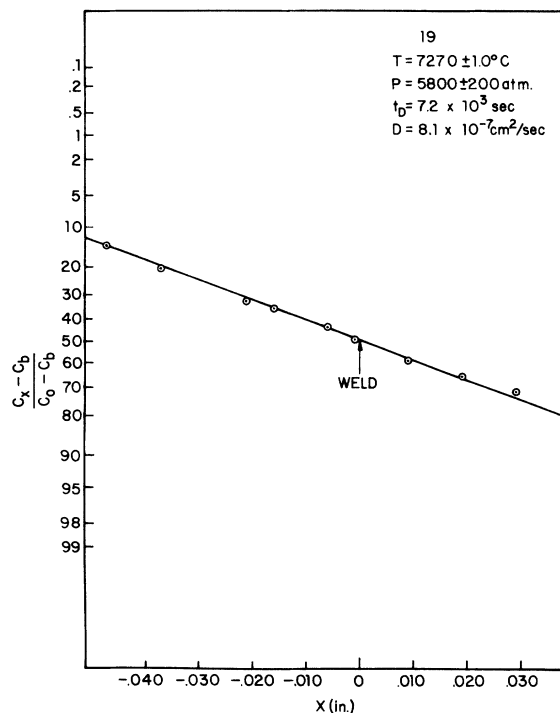


FIG. 4. Plot of concentration ratio versus distance from weld on probability paper.

vation volume" from the relationship

$$\Delta V = -RT \left(\frac{\partial \ln D}{\partial P} \right)_T \quad (5)$$

[where ΔV is the activation volume (cm^3/mole), D the diffusivity (cm^2/sec), P the pressure (atm), and R the gas constant ($\text{cm}^3\text{atm}/\text{mole}^\circ\text{K}$)] yields activation volumes of $5 \pm 1 \text{ cm}^3/\text{mole}$ and $8 \pm 1 \text{ cm}^3/\text{mole}$ at 889 and 1000 $^\circ\text{K}$, respectively. Combining these results with results from low-temperature measurements^{1,2} (i.e., zero activation volume) indicates that the pressure dependence of carbon diffusion in α -iron may be described by a *temperature-dependent* activation volume.

Alternatively, we may assume, as previously suggested,⁴ that the pressure and temperature dependence of diffusion of carbon in α -iron may be described by the equation

$$D(P, T) = 0.008 \exp \left(- \frac{19800}{RT} \right) + 2.2 \exp \left(- \frac{29300 + P\Delta V_2}{RT} \right), \quad (6)$$

where ΔV_2 is the pressure dependence of the high-temperature-mechanism's activation energy.

The first term on the right-hand side of Eq. (6) represents the temperature and zero-pressure dependence of carbon migration in α -iron at low temperatures as determined by relaxation measurements.^{1,2} The second term on the right-hand side of Eq. (6) is assumed to represent the temperature and pressure dependence of carbon migration in α -iron via a second diffusive mechanism which becomes operable at high temperatures and was previously used to explain the non-Arrhenius behavior of the diffusivity of this system.⁴ Re-

TABLE III. Summary of diffusion data.

	$T_{\text{anneal}} (^\circ\text{C})$	$t_D (\text{sec})$	$P (\text{atm})$	$D (\text{cm}^2/\text{sec})$
9	727.5 \pm 1.5	3.6 $\times 10^3$	4420 \pm 50	7.6 $\times 10^{-7}$
12	727.3 \pm 1.0	5.4 $\times 10^3$	5200 \pm 400	9.5 $\times 10^{-7}$
14	727.5 \pm 3.0	3.6 $\times 10^3$	2890 \pm 100	10.7 $\times 10^{-7}$
15	721.0 \pm 1.0	7.2 $\times 10^3$	4340 \pm 100	6.8 $\times 10^{-7}$
16	727.0 \pm 1.0	3.6 $\times 10^3$	110 \pm 5	13.2 $\times 10^{-7}$
17A	727.0 \pm 1.0	7.2 $\times 10^3$	2000 \pm 50	10.4 $\times 10^{-7}$
17B	727.0 \pm 1.0	7.2 $\times 10^3$	2000 \pm 50	13.2 $\times 10^{-7}$
19	727.0 \pm 1.0	7.2 $\times 10^3$	5800 \pm 200	8.1 $\times 10^{-7}$
18A	727.0 \pm 1.0	7.2 $\times 10^3$	2400 \pm 100	9.4 $\times 10^{-7}$
18B	727.0 \pm 1.0	7.2 $\times 10^3$	2400 \pm 100	9.2 $\times 10^{-7}$
20A	616.0 \pm 0.5	9.0 $\times 10^3$	133 \pm 5	2.32 $\times 10^{-7}$
20B	616.0 \pm 0.5	9.0 $\times 10^3$	133 \pm 5	2.45 $\times 10^{-7}$
21A	616.0 \pm 0.5	9.0 $\times 10^3$	4500 \pm 100	1.95 $\times 10^{-7}$
21B	616.0 \pm 0.5	9.0 $\times 10^3$	4500 \pm 100	1.84 $\times 10^{-7}$
22A	616.0 \pm 1.0	8.94 $\times 10^3$	5400 \pm 200	1.62 $\times 10^{-7}$
22B	616.0 \pm 1.0	8.94 $\times 10^3$	5400 \pm 200	1.78 $\times 10^{-7}$
23A	550.0 \pm 1.0	5.04 $\times 10^4$	5300 \pm 300	6.20 $\times 10^{-8}$
23B	550.0 \pm 1.0	5.04 $\times 10^4$	5300 \pm 300	6.20 $\times 10^{-8}$

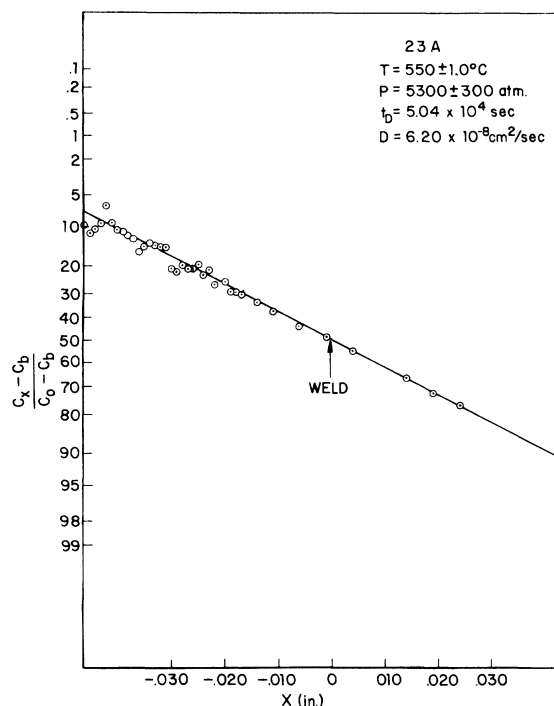


FIG. 5. Plot of concentration ratio versus distance from weld on probability paper.

arranging Eq. (6) we obtain

$$Q_2 + P\Delta V_2 = -RT \ln F = -RT \ln \left(\frac{D(P, T) - 0.008 e^{19800/RT}}{2.2} \right), \quad (7)$$

where Q_2 is the activation energy for diffusion by the second mechanism and F is defined by Eq. (7). A plot of $-RT \ln F$ as a function of pressure is shown in Fig. 8. The data plotted include two measurements made at 823 $^\circ\text{K}$ and 5.3 kbar as well as the measurements made at 889 and 1000 $^\circ\text{K}$ previously mentioned. A straight line drawn through these data yields a *temperature-independent* activation volume of $10 \pm 3 \text{ cm}^3/\text{mole}$ and an intercept value for Q_2 of 29.3 kcal/mole. This value of Q_2 is in excellent agreement with the previous measurement.⁴

The experimental limit of error reported for ΔV and ΔV_2 were obtained from Eqs. (5) and (7), respectively, and standard techniques of experimental error analysis.⁹

The pressure and temperature range of this experiment does not permit us to determine which of these two approaches is the most appropriate for this system.

The activation volumes obtained in this experiment are in disagreement with the theoretical volumes calculated by Keyes¹⁰ (1.28 cm^3/mole) and

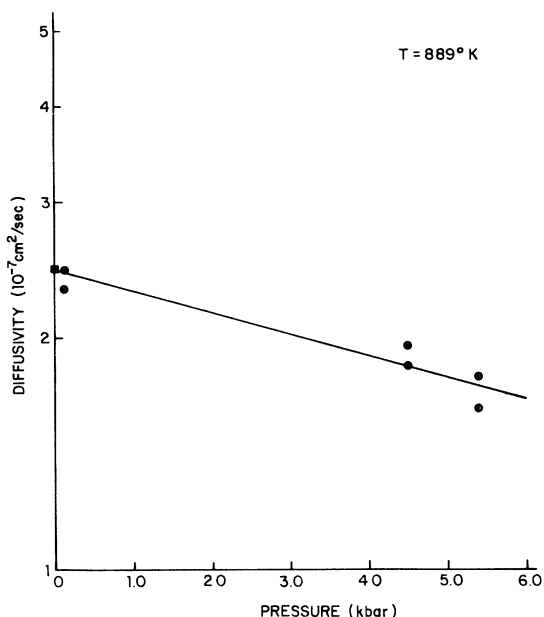


FIG. 6. Pressure dependence of the diffusion of carbon in α -iron at 889 °K.

Temkin¹¹ (0.24 cm³/mole). Nevertheless, it seems clear that at high temperatures, diffusion of carbon in α -iron decreases with increasing pressure.

Of some interest are the results of investigations by Hilliard and Cahn,¹² Nilan¹³ and Hilliard and Tully.¹⁴ Hilliard and Cahn¹² have reported activation volumes for austenite decomposition of 0.6 cm³/mole and 9.5 cm³/mole for high-purity iron-carbon alloys and commercial steel, re-

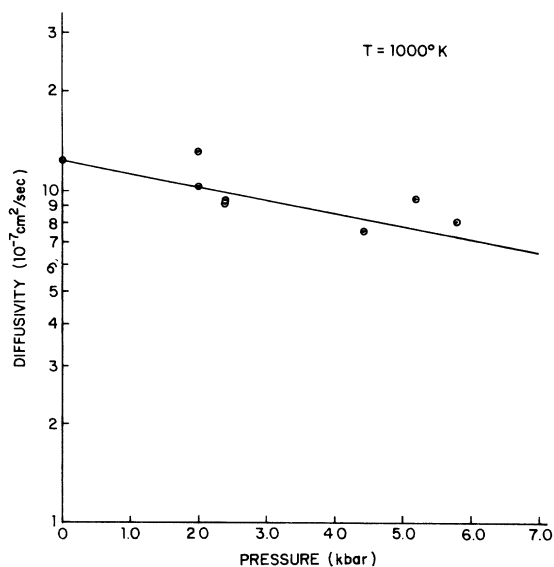


FIG. 7. Pressure dependence of the diffusion of carbon in α -iron at 1000 °K.

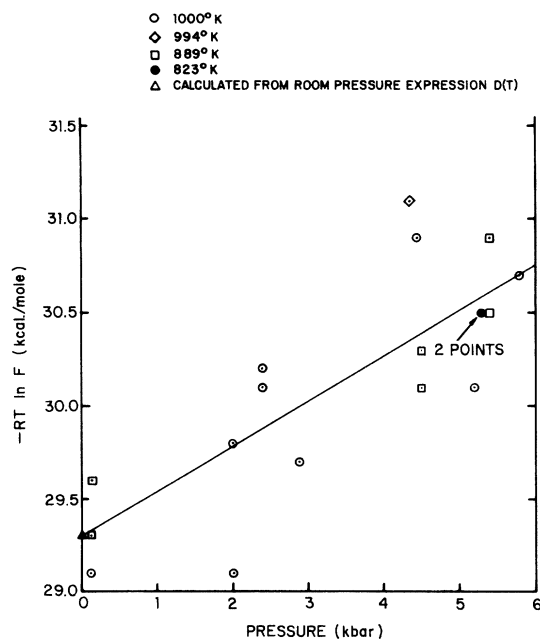


FIG. 8. Pressure dependence of the diffusion of carbon in α -iron using the two-mechanism model of Eq. (7).

spectively, at 873 °K. Hilliard and Tully,¹⁴ using hardness measurements to determine the concentration profiles, obtained an activation volume of about 1 cm³/mole for carbon diffusion in austenite. Nilan¹³ obtained an activation volume for austenite decomposition of 7 cm³/mole at 753 °K. Two of the three measurements of austenite decomposition at high pressure give activation volumes which are in reasonable agreement with the values reported here for carbon diffusion in α -iron. The smaller activation volume for austenite decomposition obtained by Hilliard and Cahn¹² from a high-purity specimen was calculated using a pearlite growth rate estimated from the data of Frye, Stansbury, and McElroy¹⁵ for a similar steel. The larger volume found in the commercial steels by Hilliard and Cahn¹² were derived from experimentally determined growth rates at room pressure and 34 kbar.

The reported activation volumes for austenite decomposition^{12,13} agree more closely with the activation volume for diffusion of carbon in α -iron than with the activation volume for diffusion of carbon in austenite.¹⁴ This result suggests that carbon diffusion in α -iron may play an important role in austenite decomposition kinetics as suggested in the ferrite-gap model of Darken and Fisher.¹⁶

SUMMARY

(i) A large pressure dependence for diffusion of

carbon in α -iron was measured for temperatures above 823 °K. This result contrasts sharply with the lack of pressure dependence obtained by relaxation measurements at low temperatures.

(ii) Analysis of the data in accordance with the empirical approach of Eq. (5) suggests a temperature-dependent activation volume varying from 5 cm³/mole at 889 °K to 8 cm³/mole at 1000 °K.

(iii) Analysis of the data in accordance with the two-mechanism model proposed in Ref. 4 suggests a temperature-independent activation volume of 10 cm³/mole for high-temperature-diffusion mechanism.

ACKNOWLEDGMENTS

The authors are indebted to Dr. Thomas E. Davidson for his helpful comments and the use of his high-pressure equipment, Dr. Lawrence V. Meisel for his helpful comments, David P. Kendall for calibration of the strain-gauge pressure bridge, and Joseph W. Hart for technical assistance. The Battelle iron was provided through the kind offices of the American Iron and Steel Institute subcommittee for pure iron, Dr. K. J. Blickwede, Chairman.

¹A. J. Bosman, P. E. Brommer, and G. W. Rathenau, *Physica* **26**, 533 (1960); **23**, 1001 (1957).

²J. Bass and D. Lazarus, *J. Phys. Chem. Solids* **23**, 1820 (1962).

³R. P. Smith, *Trans. AIME* **224**, 105 (1962).

⁴C. G. Homan, *Acta Met.* **12**, 1071 (1964).

⁵C. G. Homan and J. F. Cox (unpublished).

⁶H. M. Strong, in *Progress in Very High Pressure Research*, edited by F. P. Bundy, W. R. Hibbard, Jr., and H. M. Strong (Wiley, New York, 1961), p. 182.

⁷F. Simon, *Trans. Faraday Soc.* **33**, 65 (1937).

⁸L. Salter, *Phil. Mag.* **45**, 369 (1954); J. Gilvarry, *Phys. Rev.* **102**, 308 (1956).

⁹J. P. Nickol, H. F. Meiners, K. H. Moore, and W. Eppenstein, *Analytical Laboratory Physics* (Edwards,

Ann Arbor, Mich., 1956).

¹⁰R. W. Keyes, *Solids Under Pressure* (McGraw-Hill New York, 1963), p. 80.

¹¹D. Ye. Temkin, *Fiz. Metal. Metalloved.* **29**, 589 (1970).

¹²J. E. Hilliard and J. W. Cahn, in Ref. 6, p. 109.

¹³T. G. Nilan, *Trans. AIME* **239**, 898 (1967).

¹⁴J. E. Hilliard and W. R. Tully, ASD Technical Report No. TDR-16-21, Pt. 1, 1961 (unpublished).

¹⁵J. F. Frye, E. E. Stansbury, and D. L. McElroy, *Trans. AIME* **167**, 219 (1953).

¹⁶L. S. Darken and R. M. Fisher, *Decomposition of Austenite by Diffusional Processes* (Interscience, New York, 1962), p. 249.

Nearly-Free-Electron Susceptibility of Noble Metals*

E. Borchi and S. De Gennaro

Istituto di Fisica dell'Università, Firenze 50125, Italy

(Received 11 February 1972)

Theoretical calculations of the magnetic susceptibility of solid and liquid noble metals are presented. The effective shape of the Fermi surface of solid metals is taken into account by using the simple "eight-cone" model by Ziman. The interference function of liquid metals is evaluated according to the procedure given by Ashcroft and Lekner. A model potential recently proposed by the authors allows completion of the calculations. We find that, when electron correlations are taken into account, good agreement with the available experimental data generally results. The resulting estimates of the shift in susceptibility on melting are also confirmed by experiment.

I. INTRODUCTION

Recently tractable expressions for the magnetic susceptibility of simple metals have been obtained by many authors through the use of the pseudopotential formalism.¹⁻⁵ We have shown in a preceding paper⁶ the applicability of these expressions to noble metals also, for which some reliable pseudopotentials exist⁷⁻¹⁰; we have also carried out a simple calculation of the nonoscillatory diamagnetic susceptibility of the noble metals Cu, Ag, and Au.

In this paper we present the results of a more complete calculation of the nonoscillatory magnetic susceptibility of solid and liquid metals Cu, Ag, and Au. While for the liquid metals the calculation does not offer any trouble once accurate pseudopotentials and the liquid-structure factor are known, for the solid metals some difficulties arise because of the distorted Fermi surface. Actually, as is well known, the Fermi surface of the solid noble metals is so much distorted from a spherical shape as to contact the (111) faces of the Brillouin zone.¹¹